



Targeting the cancer cell cycle by cold atmospheric plasma

O. Volotskova¹, T. S. Hawley², M. A. Stepp³ & M. Keidar¹

SUBJECT AREAS:

PLASMA PHYSICS

CANCER

BIOPHYSICS

CELL CYCLE

¹Dept. Of Mechanical and Aerospace Engineering, The George Washington University, SEAS, 801 22nd St. NW, Phillips Hall 735 Washington, DC 20052, ²Flow Cytometry Core Facility, The George Washington University 2300 I St. NW, Ross Hall 118 Washington, DC 20037, ³Dept. Of Anatomy and Regenerative Biology, The George Washington University, SMHS, 2300 I St. NW, Ross Hall 226C Washington, DC 20037.

Received
24 May 2012

Accepted
22 August 2012

Published
6 September 2012

Correspondence and requests for materials should be addressed to O.V. (olyanv@gwu.edu) or M.K. (keidar@gwu.edu)

Cold atmospheric plasma (CAP), a technology based on quasi-neutral ionized gas at low temperatures, is currently being evaluated as a new highly selective alternative addition to existing cancer therapies. Here, we present a first attempt to identify the mechanism of CAP action. CAP induced a robust ~2-fold G2/M increase in two different types of cancer cells with different degrees of tumorigenicity. We hypothesize that the increased sensitivity of cancer cells to CAP treatment is caused by differences in the distribution of cancer cells and normal cells within the cell cycle. The expression of γ H2A.X (pSer139), an oxidative stress reporter indicating S-phase damage, is enhanced specifically within CAP treated cells in the S phase of the cell cycle. Together with a significant decrease in EdU-incorporation after CAP, these data suggest that tumorigenic cancer cells are more susceptible to CAP treatment.

The complex nature of cancer makes it difficult to develop effective treatments. Targeted cancer therapies are defined as substances or methods that block tumor growth by interacting with specific molecules or that focus on treatments to cancer specific molecular and cellular changes. Several targeted cancer therapies exist today. Examples include chemotherapy, radiotherapy and molecularly targeted drugs^{1–3}. One way to target cancer cells is to interfere with the cell cycle. Cancer cells proliferate at a faster rate than normal cells⁴. Combination therapies are proved to be most effective; they impact cancer cell biology at multiple signal transduction pathways resulting in a synergetic effect. The goal is to trigger cells to execute what has been referred to as “the cell death pathway” or apoptosis. A major hurdle in treating cancers is preserving surrounding normal tissue while inducing cell death within cancer cells within a tumor. While progress is being made at developing treatments that are selective for cancer cells, cancer treatment induced damage to normal cells within tissues remains a major problem in oncology.

Recently, it was reported that newly developed cold atmospheric or non-thermal plasmas (CAPs) could be used as an alternative therapies for cancer^{5,6}. It was shown *in vivo* that tumor size can be decreased when CAP treatment was applied locally. Analysis of the CAP effect *in vitro* revealed that cancer cells die due to apoptosis. It was reported early that the reactive oxygen species (ROS) are the major players in the cell response to CAP treatment *in vitro* and *in vivo*. Additional effects of cold atmospheric plasmas on the living tissue at various levels were shown: plasma sterilization, improvement in wound healing, cell migration changes, changes in the protein expression^{7–12}. The variety of different effects of plasma can be explained by the complex chemical composition of CAP and variations in the way that CAP is generated. In fact, CAP is a cocktail containing variety of ROS, reactive nitrogen species, charge particles, UV etc. This variety leads to the myriad of effects mentioned above. While most studies tackle individual effects related to particular application of interest, there are few studies that correlate cell responses and intracellular dynamics. While we have looked at CAP effects on integrin mediated cell adhesion and signaling in normal and skin cancer cells, our studies only begin to address the mechanism of plasma action on cancer cells remains elusive.

In this study, we set out to correlate the changes seen in cell motility observed previously¹³ in normal primary skin cells with viability and cell cycle progression under CAP treatment. We hypothesize that cancer cells are more susceptible to the effects of CAP because a greater percentage of cells are in the S phase. To test our hypothesis, we used normal cells derived from mouse skin as well as two mouse skin cancer cell lines. The skin is the largest human organ and includes 15–20% of total body mass. The outer layer of the skin, the epidermis, is composed primarily of keratinizing stratified squamous epithelial cells. Two competing processes sustain the thickness of the epidermis: proliferation and terminal differentiation of keratinocytes; both processes are driven by specific signaling pathways. Disturbances of cell-matrix, cell-cell adhesion, or terminal differentiation can lead to homeostatic imbalance in various diseases including skin cancers. Reduced terminal differentiation of skin cells

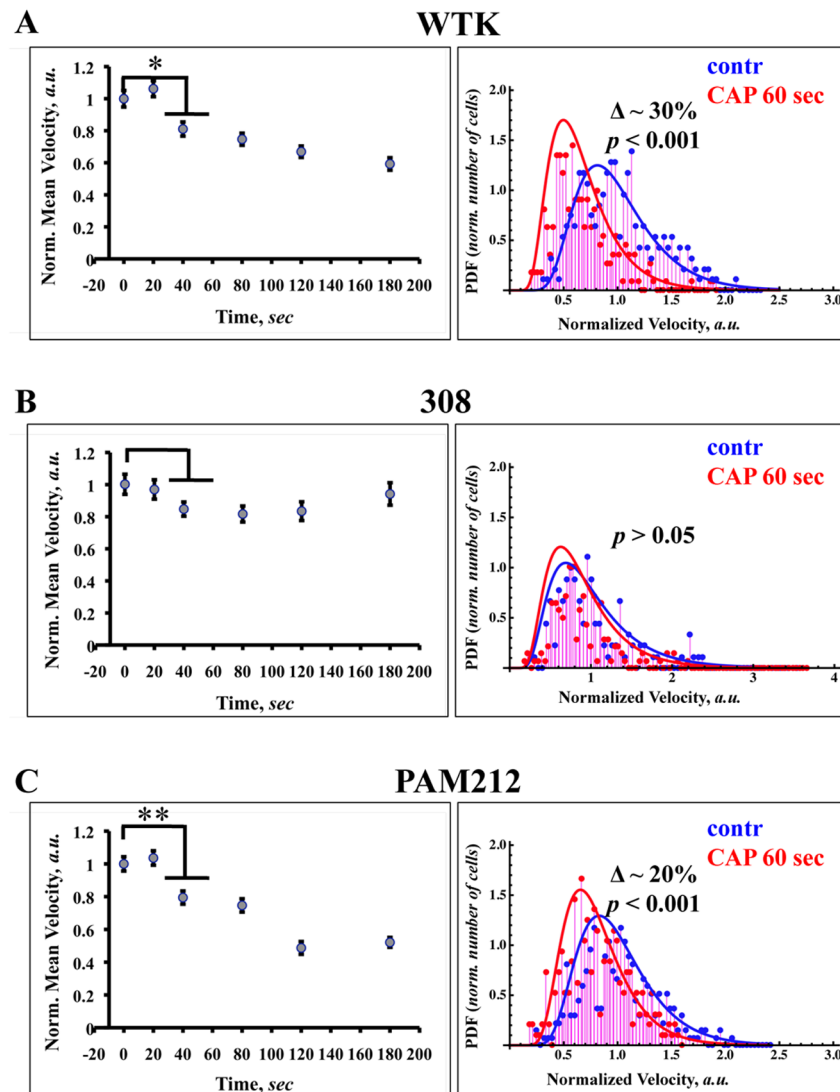


Figure 1 | CAP effect on the cell migration and velocity distribution among the chosen cell population. The dependence of the cells migration rates on the length of the CAP treatment from 0 to 180 seconds are shown for WTK, 308 and PAM 212 cells (Figure 1A–1C, left panel). SEM (standard error of mean) is shown with an error bars. For each time point ~ 50 – 60 cells were analyzed. The difference between groups were considered statistically not significant for p -value > 0.05 (no mark) and for p -value < 0.05 (single star), p -value < 0.01 (double star) and p -value < 0.001 (triple star) are considered significant. The probability distribution functions (PDF) of the cell migration rates (distribution of the cell velocities) for untreated cells (control, blue) and cells treated with cold atmospheric plasma for 60 seconds (plasma treated, red) are shown for WTK, 308 and PAM 212 cells (Figure 1A–1C, right panel). The experimental data (~ 250 cells of each cell type were analyzed for each condition) is fitted with inverse Gaussian distributions.

allows the cells to continue proliferating and is a common feature of skin cancers^{14,15}. Here we compare CAP responses of normal primary mouse keratinocytes with those of two well studied mouse skin cancer cell lines that were derived from normal mouse keratinocytes. While the two cell lines consist of transformed keratinocytes, they vary in their ability to induce tumors when injected into mice, a property referred to as tumorigenicity. One line (308) generates benign tumors called papillomas whereas the other (PAM212) generates carcinomas^{16–18}.

We report that CAP treatment induces a delay in progression of skin cancer cells through the cell cycle by increasing the numbers of cells at the G2/M checkpoint ~ 24 hours after treatment and that this delay correlates with increased expression of γ H2A.X (pSer139) and DNA replication decrease in the S phase of the cell cycle. γ H2A.X (pSer139) is an oxidative stress reporter indicating S-phase damage. These data can be exploited to ensure that therapies developed using CAP in combination with other therapies induce optimal results and minimize damage to healthy tissues.

Results

CAP effect on the cell migration and velocity distribution among the chosen cell population. First we identified how CAP affects migration of normal and transformed epithelial cells. The right panel of the Figure 1A – C shows the dependence of cell migration rates on the length of the CAP treatment from 0 to 180 seconds. For each time point ~ 50 – 60 cells were analyzed. The cell velocities/migration rates and cell numbers were normalized. Statistical analysis of the data showed that wild type keratinocytes (Figure 1A) and PAM 212 cells (Figure 1C) have a statistically significant change in the migration rates beginning 40 seconds of CAP treatment. The migration rates for WTK and PAM212 cells after 60 seconds of CAP is $\sim 30\%$ and $\sim 20\%$ less than untreated cells; these changes are well identified by velocity distribution function of the cells and become even more statistically significant. The left panel of the Figure 1A–C shows the probability distribution functions (PDF) of the cell migration rates (distribution of cell velocities) for untreated cells (control, blue) and cells treated with cold atmospheric plasma for

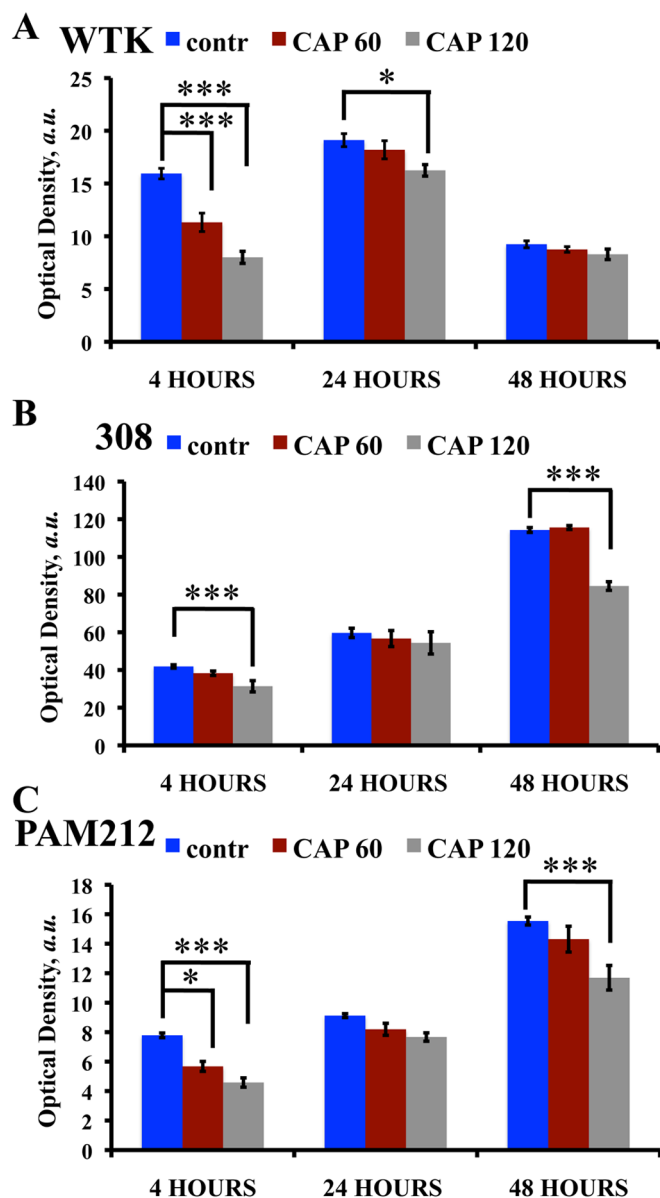


Figure 2 | Cell viability studies in two threshold regimes. MTT assay was performed on: (A) wild type keratinocytes (WTK), (B) 308 cells (papilloma) and (C) PAM212 cells (carcinoma). Control (not treated) is shown in blue, CAP treated for 60 seconds – in red and CAP treated for 120 seconds – in grey cells at 0, 4 and 24 hour time points. SEM is shown with an error bar. The experiment was repeated 3 times for each cell type and condition. Three stars denote extremely significant statistical difference (p -value < 0.001), one star – statistically significant difference (p -value < 0.05), data was considered statistically not different for p -value > 0.05.

60 seconds (plasma treated, red). The experimental data (~250 cells of each cell type were analyzed for each condition) are fitted with inverse Gaussian distribution, which describes the first passage in Brownian motion with positive drift¹⁹. For normal and transformed (PAM 212) cells, longer CAP treatments increased the reduction of cell migration. CAP treatment for ~120 seconds gave the upper threshold in the cell migration reduction for the chosen time treatment range (see inserts in Figure 1A and 1C). Unlike normal and PAM212 cells, 308 cells did not show any significant change in their migration rate after plasma treatment. It is important to note that 308 cells have very slow motility; their average velocity is approximately 10 fold less than WTK and PAM212 cells. The cell velocity distribution of WTK cells showed the most apparent

negative shift from control under the mild CAP treatment, unlike PAM212 cells. The cells were also treated with helium only for 60 seconds, no significant differences in migration rates were found (p -value > 0.05, data not shown).

Cell viability studies in two threshold regimes. The experiments presented in Figure 1 indicate that cell migration rates of normal and PAM212 cells are sensitive to CAP. By plotting the data using PDF, data show that after CAP, migration rates of normal and PAM212 cells cluster more tightly indicating reduced variability among cells within the population. To determine whether there were differences in cell viability among adhered normal WTK, 308, and PAM212 cells, an MTT assay was performed.

The MTT assay results are shown in Figure 2A – C for WTK, 308 and PAM212 cells respectively. The assay was performed 4, 24 and 48 hours after two threshold regimes of CAP treatment: 60 seconds (low threshold) and 120 seconds (upper threshold) were used to identify changes in cell viability. WTK cells viability decreased by 30% and 50% after 60 and 120 seconds of CAP treatment in ~4 hours after treatment. By 24 hours, cell viability after CAP recovers after both treatment lengths (Figure 1A). The viability of 308 cells was not changed 60 seconds of CAP treatment, but was significantly reduced after 120 seconds of CAP treatment in ~4 and 48 hours (see Figure 2B). PAM212 cells responded to CAP treatment with a 30% and 40% decrease in viability after 60 and 120 seconds respectively 4 hours after treatment. While 308 cell viability recovered 24 hours after treatment, similar to 308 cells, PAM212 cells showed reduced viability 48 hours after 120 seconds of treatment (Figure 2B, C). No viability differences were observed after 60 seconds of CAP treatment at ~24 and 48 hours for all types of cells. Based on these data, CAP treatment for 60 seconds was chosen. This treatment regime induces a change in cell migration in normal and PAM212 cells and causes no significant effect on cell viability 24 and 48 hours after treatment, thus allowing determination of the initiation of the CAP effect on the cells. So the following studies were made for 60 seconds of CAP treatment.

We also used flow cytometry to estimate the number of control (untreated) adhered cells per well for chosen time points (data not shown): 308 and PAM 212 cells expand fast: having a double-triple fold increase at each chosen time point. The numbers of normal keratinocytes adherent on tissue culture dishes do not change over time in vitro significantly. In fact, the number of normal keratinocytes decreases on the 3d day due to the onset of terminal differentiation and this fact is reflected by MTT data.

Identification of the cell cycle changes in G2/M-phase. Next we identified the CAP effects on the cell cycle of normal, 308 and PAM212 cells. Figure 3A–3C are bright-field images with 10X magnification of wild type keratinocytes, 308 and PAM212 cells morphology, respectively. Figures 3D–L are DNA content measurement of control (untreated) cells in blue, and cells treated with CAP for 60 seconds in red. The cells were analyzed in ~4 hours (Figure 3 D, E, F), ~24 hours (Figure 3 G, H, I) and ~48 hours (Figure 3 J, K, L) after 60 seconds of CAP treatment. No significant shifts in the G1 – G2 peaks positions were observed for all of the cell types. The results were analyzed with Watson (pragmatic) cell cycle model (FlowJo 7.6.5 software), which does not make any assumption about the S-phase distribution. The data were characterized by the fraction of the cells in the G2/M-phase as well as the coefficient of variation (CV) for control (untreated) and CAP treated cells. CAP induced robust G2/M–cell cycle increases in both carcinoma (Figure 3I) and papilloma (Figure 3H) cells (2-3-fold increase in ~24 hours after CAP treatment), whereas normal keratinocytes (Figure 3G) showed a more modest cell cycle increase. This change diminished in ~48 hours. The coefficient of variation (CV, a normalized measure of dispersion of a probability distribution) was used to characterize the data. For all 3 time points, wild type cells showed ~15–20% CV

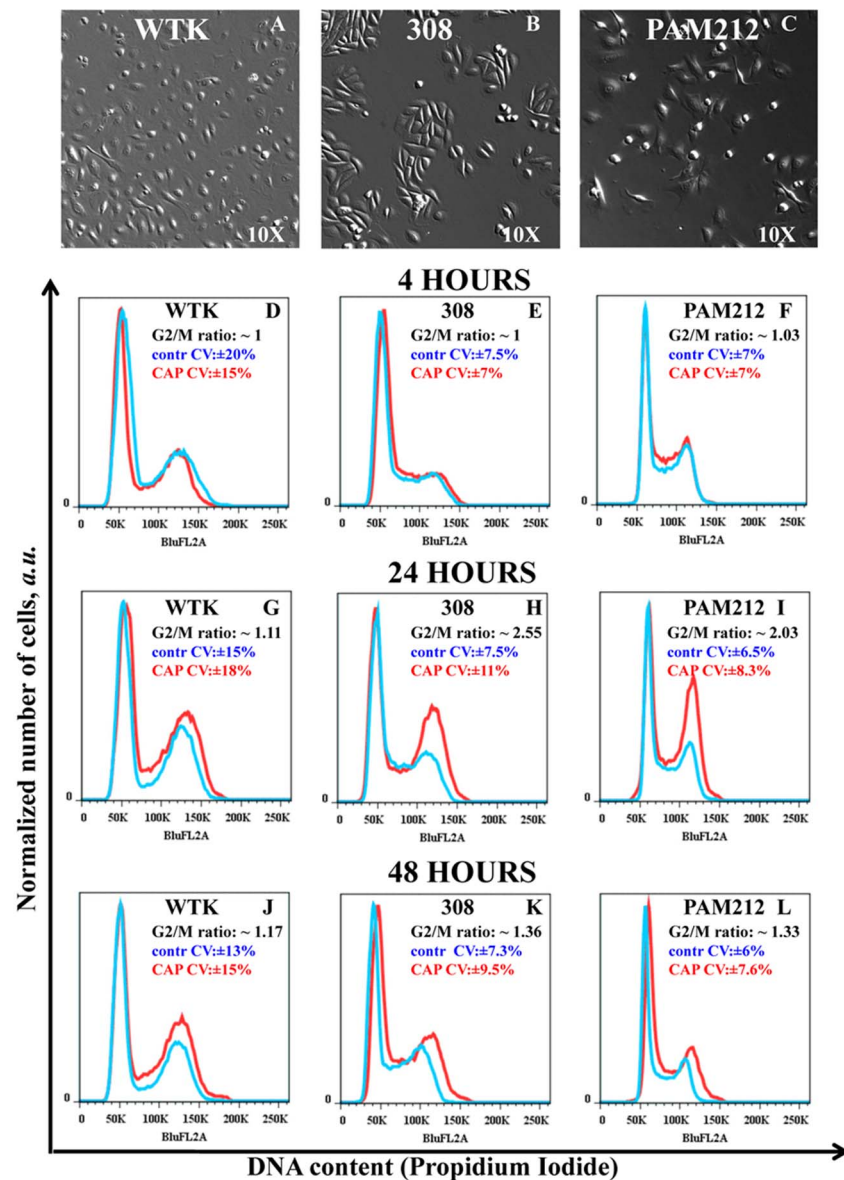


Figure 3 | Identification of the cell cycle change in G2/M-phase. Figure 3A–3C Bright-field images of wild type keratinocytes (WTK), epidermal papilloma (308 cells) and epidermal carcinoma (PAM212 cells) cells are shown with a magnification 10x. Figure 3D–3L show cell cycle studies: Propidium Iodide content (horizontal axis) and normalized number of cells (vertical axis) are shown. The controls are shown in blue and cells CAP treated for 60 seconds are in red. The ratio of the number of cells (treated to untreated) in G2/M-phase with coefficients of variation (CV, in percents) is shown in the right top corner of each figure. Figure 3D – 3F shows cell cycle measurements in ~4 hours; Figure 3G–3I in ~24 hours; and Figure 3J–3L in ~48 hours after the CAP treatment for WTK, 308 and PAM 212 cells respectively. The data is shown for ~25000–50000 cells for each experimental condition. The measurements were repeated 2–3 times.

values for the cells in G2/M-phase, while transformed cells had CV value of ~6–10%.

Studies of the cell population’s distribution during the cell cycle under CAP treatment. In order to determine if increased proliferation of the cells might result in the above observed G2/M increase 24 hours after CAP treatment, we carried out a more detailed analysis of the cell cycle. Cells were treated with the nucleotide analog EdU which is incorporated into DNA as it is being replicated. After staining EdU treated cells with a dye that binds to DNA (Propidium Iodide or PI), flow cytometry was used to assess the numbers of cells in the three distinct phases of the cell cycle (G0/G1, S, and G2/M) simultaneously for all three cell types; data are shown in Figure 4A–F. Results are presented for the time point 24 hours for the control (untreated) cells and CAP treated cells for 60 seconds. As expected, fewer

normal cells were in S phase (~10%) compared to the two cancer cell lines (transformed cells are highly proliferative): ~50% for 308 cells and ~45% for PAM212 cells. No increase in the fraction of cells in the S-phase after CAP treatment was observed for the three cell types: their number either remained the same or decreased. However, we did observe an increase in the ranging of standard deviation value of CAP treated cells in S-phase of around ~20% for all three cell types suggesting that not all cells within the population of cells responded the same to CAP treatment. While we did not see a significant difference in the numbers of cells in the S phase of the cell cycle, we did see that the number of cells in the G2/M fraction increased by ~25% for normal cells and 2- to 3-fold for transformed cells. The increase in the fraction of cells at the G2/M phase of the cell cycle is accompanied by a decrease in the number of cells in the G0/G1 fraction. This study also shows the general trend in the distribution of cells

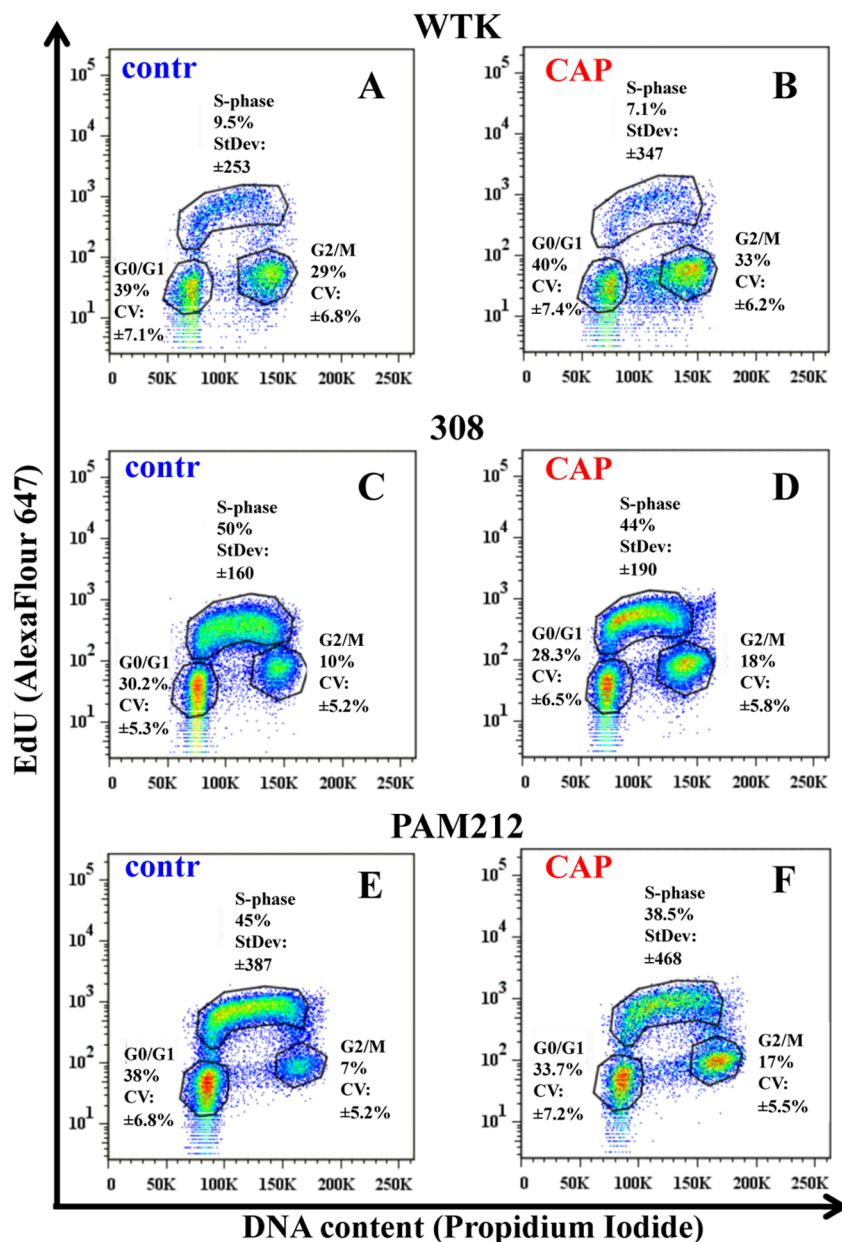


Figure 4 | Studies of the cell population's distribution during the cell cycle after CAP treatment. The detailed studies of the cell cycles for control and CAP treated for 60 seconds cells are shown. The correlation between DNA content (Propidium Iodide) and DNA-replicating cells (EdU-component) is shown for: Figure 4A, 4B – normal cells (wtk); Figure 4C, 4D – papilloma cells (308 cells); and Figure 4E, 4F – carcinoma cells (PAM212 cells) in ~24 hours after CAP treatment. Coefficient of variation (CV) was used to characterize the Propidium Iodide data (linear scale) and standard deviation (StDev) was used for EdU-data (log scale) in each phase. Fractions of the number of cells in each cell cycle phase are shown in percents. The data is shown for ~25000 cells for each experimental condition. The experiments were repeated 2–3 times.

within the cell cycle and indicates that timing of the cell cycle is different for chosen cells.

Cell synchronization for G2/M peak increase studies. We next designed an experiment to determine whether cells synchronized at the G2/M phase of the cell cycle and released would also show an increase in accumulation at the G2/M checkpoint. 308 cells were chosen for these studies because they showed a robust G2/M-peak increase after CAP treatment. On the other hand 308 cells did not express any significant changes in the migration after CAP was applied. This makes 308 cells most appropriate example to distinguish between the cell migration and the cell cycle effects of CAP. Cells were synchronized with nocodazole, a drug that interferes with microtubule polymerization and causes mitotic spindle arrest,

thereby preventing cells from entering mitosis; the effect is reversed upon its removal. The drug was removed and cells were treated by CAP in ~2 hours after removal of nocodazole. Figure 5A shows the time dynamics of the cell cycle immediately after nocodazole removal (0 hours point), at the ~4 hour time point (it is around the time of CAP treatment) and in ~24 hours after CAP treatment when G2/M-increase was observed. Figure 5B shows the detailed distribution of cells among phases of the cell cycle 24-hour time point of the cells pre-treated with nocodazole including CAP treatment. Cell synchronization did not impact the G2/M pause induced by CAP. The coefficient of variation holds ~ around 5–7%, while the fraction of the cells in G2/M-phase doubled in ~24 hours after CAP treatment of nocodazole pre-treated cells. The cell cycle of cells pre-treated with nocodazole only restored to

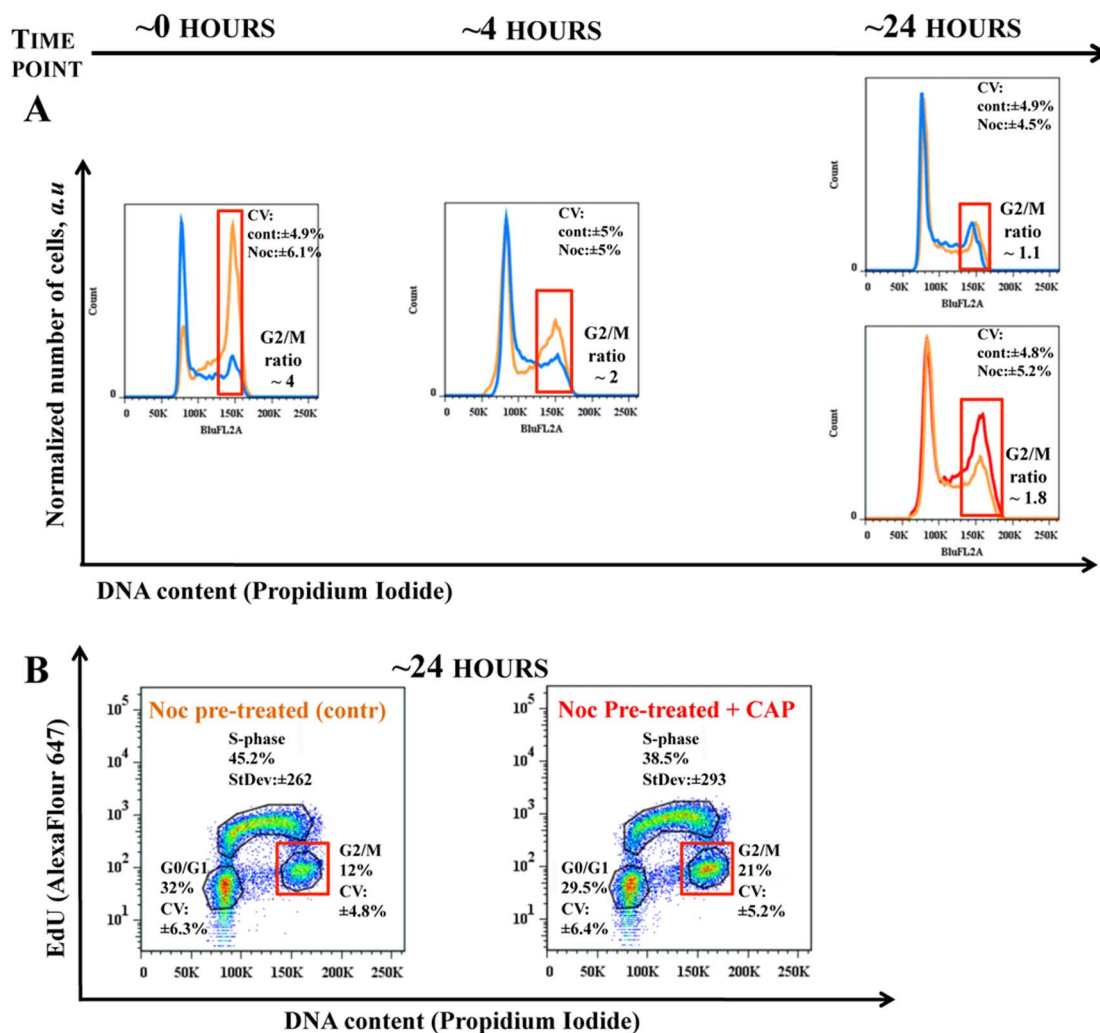


Figure 5 | Cell synchronization for G2/M increase studies. 308 cells were synchronized with nocodazole and analysis of the cell cycle was carried out for various time points. Figure 5A shows the time evolution of the 308 cells: the control cells (not treated cells) is shown in blue, the cells pre-treated with nocodazole is in orange and nocodazole pre-treated cells which were CAP treated for 60 seconds – in red. The cell cycle evolution after nocodazole removal (the state of the cell cycle for this time point is not shown). The final state of the systems control (not-treated cells), cells pre-treated with nocodazole only and cells pre-treated with nocodazole and treated with CAP is shown for time point ~24 hours. The change in ratio between G2/M fractions of the cells at each experimental condition is marked with a red square. Figure 5B shows detailed cell cycle studies of 308 cells for chosen time point ~24 hours. The DNA content (Propidium Iodide, linear scale) and DNA-replicating cells (EdU-component, log scale) characterized by CV (in percents) and StDev (arb. units) values, respectively. The data is shown for ~25000 cells. The measurements were repeated 2–3 times.

control (not treated) cells profile in ~24 hours. The variation of the data spread for cells in S-phase for CAP treated cells was again ~20% more than cells pre-treated with nocodazole only. This data also suggested that dynamics of the cell cycle in 308 cells is rapid. Nocodazole caused ~4-fold increase in the number of cells in the G2/M phase of the cell cycle. When nocodazole is removed, by ~4 hours cells begin progressing in synchrony from G2/M to G0/G1 and the ratio of the cells in G2/M-phase falls to ~2-fold increase with the accumulated DNA-replicating cells in S-phase. Thus, we cannot conclude from this study whether or not CAP impacts cells within S phase or G2/M-phase. However, we can state that G2/M-pause after CAP occurs whether or not cells have been synchronized.

CAP targets the cell cycle. To directly test whether CAP impacts some cell-cycle phase specifically, experiments were designed to assess the expression of γ H2A.X (pSer139) at different phases of the cell cycle. Based on the earlier experimental results shown, we surmised that the G2/M-pause after CAP occurs whether or not cells have been synchronized

on cells in the S and/or G2/M phases. It was previously reported by Keidar et al. (2011) that CAP based on helium flow may induce ROS response in the cells⁵. Thus, we choose γ H2A.X (pSer139) as an oxidative stress reporter of S-phase damage. This histone comprises around ~2–25% of the evolutionarily conserved variant of histone H2A, it goes through a post-translational modifications in response to ionizing radiation, UV-light or ROS^{20,21}. It can be used in combination with EdU-labeling to determine if the oxidative stress is induced in S-phase²². Figure 6 shows the results of time sensitive 308 cell response studies to CAP treatment of 60 seconds: DNA content in cells, DNA replicating cells and γ H2A.X expression were measured simultaneously. Figure 6A shows the cell cycle dynamics (EdU/DNA content) of 308 cells immediately following and at 4 and 24 hours after CAP treatment. Note the very significant change in the S-phase signal (EdU) at ~0 and ~4 hours: almost 2-fold decrease in the median value with decrease of variation range value (see Figure 6 for detailed analysis), while still no significant changes were observed in G0/G1 and G2/M; at the ~24 hours time

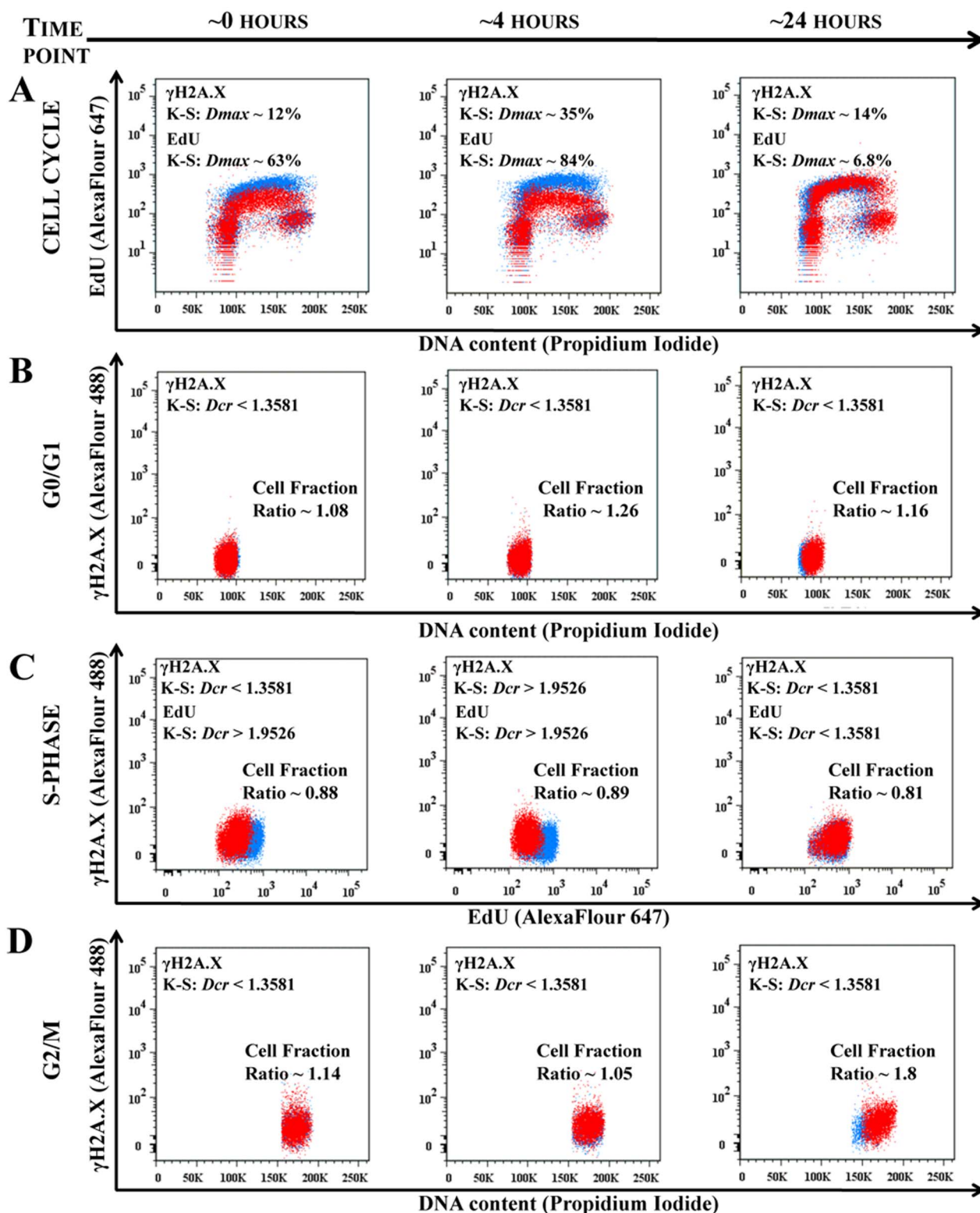
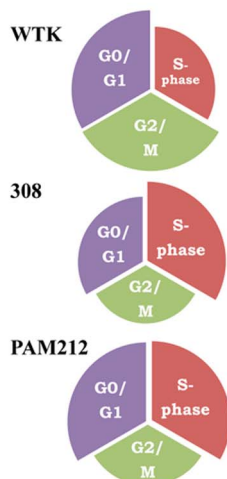


Figure 6 | CAP targets the cell cycle phase. The time sensitive studies of the 308 cells cell cycles are shown for the time points ~ 0 hour, ~ 4 hour and ~ 24 hours points after 60 seconds of CAP treatment. The control (not treated cells) is shown in blue, CAP treated cells is in red. Figure 6A shows the time evolution of the cell cycles (DNA content – vs. – DNA replicating cells) of control and CAP treated cell. The changes in EdU and γ H2A.X signals are characterized by K-S maximum difference D_{max} and D_{cr} values at the selected time point. Figure 6B shows the correlation between DNA content and γ H2A.X reporter for G0/G1 cell phase; Figure 6C shows correlation between DNA replicating cells (EdU) and γ H2A.X for 308 cells in S-phase; and Figure 6D shows correlation between DNA content and γ H2A.X for the 308 for G2/M-phase for ~ 0 , ~ 4 and ~ 24 hours time points. ~ 25000 cells are shown for each experimental condition. Changes in the fraction of cells between the control (not treated) and CAP treated cells are shown for each cell phase: cell number decreases if the ratio is less than 1. The statistical description of the signals shown in the Figure 6A is a maximum differences between two distributions in the S-phase with confidence interval 99.9%; in the Figures 6B–6D D_{cr} – value is shown: $D_{cr} < 1.3581$ ($p > 0.05$) is considered not statistically significant and $D_{cr} > 1.9526$ ($p < 0.001$) is extremely statistically different²⁹.



A DISTRIBUTION OF THE CELL POPULATIONS DURING THE CELL CYCLE



B TARGETING CELL CYCLE BY CAP

PLASMA AFFECTS THE CELL MIGRATION IN G0/G1 AND POSSIBLY PART OF S-PHASE

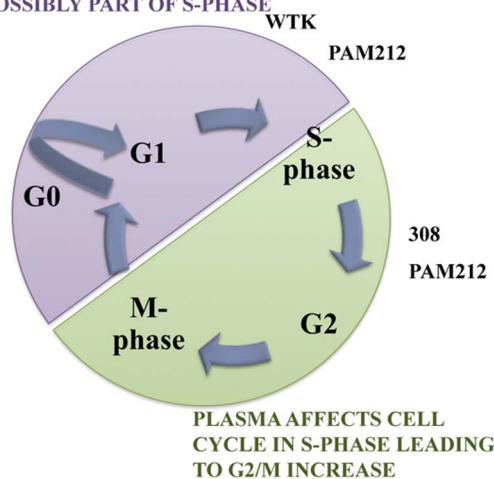


Figure 7 | The schematic model of the CAP impact on the cell cycle. Figure 7A is the schematic representation of the cells distribution during the cell cycle phase for analyzed types of cells: WTK, 308 and PAM212. Figure 7B is schematic of the CAP affect on the cell cycle with consequent cell response.

point the S-phase recovered and the number of cells in G2/M 24 hours after CAP treatment was increased. Figures 6B–6D represents the correlation between γ H2A.X signal and DNA content in G0/G1-phase (B); with EdU incorporation to highlight S-phase cells (C), and with DNA content to highlight cells in G2/M-phase (D). There were no significant differences in γ H2A.X (pSer139) expression in cells at G0/G1 at any time point (Figure 6B). There was an increase in γ H2A.X (pSer139) expression (maximum difference $D_{max} \sim 30\%$ at time point 4 hours) correlated with ~ 2 -fold decrease in the EdU-signal in cells mostly in the S phase immediately (0 hours) and 4 hours after CAP treatment (Figure 6C). Differences in γ H2A.X (pSer139) expression were less apparent 24 hours after CAP treatment: G2/M phase showed some increased variation of γ H2A.X (increased ranging value of standard deviation with some increase in the median value) at the time point ~ 24 hours, which correlated with the increase of the number of cells (G2/M increase, corroborating earlier observations, Figure 6D).

Discussion

It has been shown at the cellular level that cold atmospheric plasma (CAP) could be used as alternative tool for cancer therapy. The effect of CAP on cells depends on the length of the time cells are treated with a specific power, the chemical composition (helium flow based jet), and the number of cells within the population treated that are in the S-phase. Normal skin cells are less likely to be in S-phase of the cell cycle compared to cancer cells. Regardless, their migration rate and viability are transiently reduced by mild CAP treatment. Normal skin cells do not induce tumors when injected into mice; two different cancer-causing cell lines do cause tumors¹⁸. More tumorigenic cell line (PAM212), like normal cells, also shows reduced migration rates and viability after mild CAP treatment but the other cell line (less tumorigenic papilloma cells) shows neither reduced migration rates nor reduced cell viability. To determine the underlying causes of these differences, detailed cell cycle assessments were conducted on the CAP treated cells. These data show that CAP affects all stages of the cell cycle, however depending on the phase of the cell cycle in which a cell exists the outcome of the CAP treatment or the cell response is different. We track only those cells that do not undergo mitosis over the 16 hr and 40 min time period; the cells are subjected to time lapse were most likely in G0/G1 or S-phase. Experiments

using dermal fibroblasts and epithelial cells suggest that differences in integrin expression and/or activation (conformational changes on the cell surface) cause the cell migration effects induced by CAP^{23,24}. The migration rate of 308 cells is very slow (~ 10 -fold less) compared to normal keratinocytes and PAM212 cells. Despite the fact that CAP had no effect on cell migration in 308 cells, our detailed analyses of the cell cycle and expression of γ H2A.X (pSer139) in these cells shows that they do respond to CAP treatment. Like normal cells and PAM212 cells, 308 cells undergo transient G2/M pause after CAP.

The experiments presented show that the phosphorylation of histone γ H2A.X was most evident in cells in S-phase (median rise up to $\sim 35\%$); however, a not-quite mathematically significant increase was also observed in G2/M. The increase of γ H2A.X expression correlated with an abrupt decrease in the median value of EdU signal that started immediately after CAP treatment and continuing at the 4-hour time point. Thus, CAP causes reduction in progression of cells through S phase (DNA-replication slows down), induces oxidative damage to DNA, indicated by phosphorylation of histone γ H2A.X on serine residue 139, leading to the accumulation of cells at the G2/M checkpoint caused by the DNA damage.

The kinetics of γ H2A.X phosphorylation suggests that CAP treatment most likely is not related to Double-Strand Breaks²⁵ confirming earlier experimental findings⁶. It has also been shown that phosphorylated H2A.X forms nuclear foci at the sites of stalled replication forks in response to exposure of S-phase cells to UV radiation and chromatin changes or modifications play a role in the replication block pathway²⁶. The spectral analysis of CAP jet showed that most of species were excited at the UV range (280–450 nm), providing a possible explanation for induction of S-phase damage, however ROS stresses has to be taken into account as well¹³. With the mild CAP treatment, only a $\sim 10\%$ decrease in the number of S-phase cells was detected, so this treatment (as MTT also showed) does not kill skin cells effectively. But as shown on the Figure 2, increasing the treatment length to 120 seconds decreases the viability of the cells. The fact that most of the reduction appeared in ~ 48 hours could be explained by the initiation of apoptotic pathway in those cells in S-phase which subsequently did not recover. This is in the agreement with results previously shown by Yan et al⁷. In ~ 24 hours, restoration of the S-phase of the cell cycle was accompanied by an increase in



G2/M peak, indicating that the CAP treated cells progressed into the G2/M phase. We did not observe significant differences in G2/M in normal keratinocytes where ~10–15% of cells within the population are in the S-phase; ~40–50% of cancer cells are in the S-phase.

Figure 7 shows the correlation of the CAP-induced effects with various types of cells. The 308 cells are different in many ways from the PAM212 cells despite that fact that both cells lines arose from mouse keratinocytes in the same laboratory at the NCI at the NIH. It would be necessary to study in detail several additional sets of normal and transformed cells before we could definitively conclude that increased susceptibility to CAP correlates with tumorigenicity of the cells. The progression of these two cell types through the cell cycle is different and one should take into account that the strength of the treatment effect correlates with the time point chosen for analysis. However, the data we produce here goes a long way towards proving that mild CAP impacts DNA synthesis and causes a transient cell cycle pause at the G2/M phase of the cell cycle; and that overall CAP impact on the migration rates, viability and cell cycle increases on the cancer cells as they are more tumorigenic (see Figure 1,2,3). It's important to note here that other cancer cell lines and *in vivo* models tested with the similar CAP treatment conditions showed some variation in resistance and timing for the cell cycle effects, which is determined by their differences^{5,6}.

The overall effect of CAP on the cells will be a combination of various physical phenomena including the interaction of electromagnetic radiation (UV/VUV, visible light, IR, high-frequency electromagnetic fields, etc.) with ions, electrons, and reactive chemical species (ROS or RNS). It is not clear yet what particular component induces oxidative stresses in cells. CAP could directly and/or indirectly cause formation of intracellular ROS. From our data and others, it appears that *in vivo*, we will face a cumulative or synergetic effect of CAP as discussed by Vandamme *et al.*⁶. Our data show that depending on the phase a cell is within the cell cycle and the adhesion of that cell to the substrate, CAP effect varies. In more advanced biological systems (tissues and organs) which consist of networks of communicating and interacting cell types, the effect of CAP will undoubtedly be more complicated.

Methods

One should note that only attached cells were analyzed, since it is known that keratinocytes *in vitro* tend to have floaters and it is impossible to include them in cell motility analysis. The migration rates in the presented data are the results of individual cell tracking (not a sheath) and flow cytometric cell analysis techniques enable characterization of large numbers of individual cells.

Cell culture. Wild Type Keratinocytes cells (WTK, the procedures used to isolate and cultivate cells from mice were authorized and approved by the GWUMC Institutional Animal Care and Use Committee; wt mice (BALB/c) were obtained from NCI-Frederick¹⁶, 308¹⁷ and PAM 212¹⁸ cell lines were obtained from NIH NCI Dr. S.H. Yuspa Group.

Cell culture dishes were pre-coated with Fibronectin/Collagen I solution (FN/CN I, 10 µg/ml fibronectin from BD Bioscience, Pasadena, CA, cat# 354008/1% collagen type I from Advanced BioMatrix, San Diego, CA, Part# 5005) for 20 min and incubated at 37°C. Firstly cells were plated in special plating medium and incubated at 37°C for 28–20 hours, then washed twice with PBS (Dulbecco's Phosphate Buffered Saline without Calcium or Magnesium, Lonza cat# 17-512F) and incubated in Low-Calcium Medium for ~24 hours at 37°C. Low-Calcium Medium with calcium concentration ~0.05 mM was prepared from 500 ml Minimum Essential Medium (S-MEM, Invitrogen Lot# 652978, Formula# 98-0216OJ) with 1.1 ml Pen-Strep Solution (Invitrogen, Gibco, cat# 15140) and 36 ml of Chelexed Fetus Bovine Serum. High-Calcium Medium with calcium concentration ~1.4 mM was made from Low-Calcium Medium with addition of 2.2 ml of Calcium Chloride 0.296 M. The plating medium was prepared by mixing High-Calcium with Low-Calcium Media in the ratio 1:6. Cell confluence ~50–60% was used for cell tracking studies, for other experiments the confluence was ~70%.

CAP (cold atmospheric plasma) jet. The cold atmospheric plasma jet is the dielectric barrier discharge in helium that is described elsewhere²⁷. The working parameters were: the output voltage was about 4.5–5 kV, the frequency ~13 kHz, the helium flow rate ~10 L/min. The distance between the jet outlet and culture plate was kept about 20 mm. The average jet dose at the distance 20 mm from jet outlet ~0.8 J/sec cm² was determined from (Shashurin APL 2009, 28). The CAP jet represents itself the streamer "plasma bullet" propagating along with gas flow with the velocity is about

2×10^6 cm/sec²⁷. Plasma density in the streamer head was about $5-10 \times 10^{13}$ cm⁻³²⁸. The ionized nitrogen species and highly reactive oxygen radicals are presented in the CAP spectrum¹³. We used helium as a control to establish the experimental conditions: the initial depth of the media ~2 mm would not allow desiccation of the cells during the chosen CAP treatment times. All experiments with cold plasma were conducted on the 3rd day after cell plating. Epithelial cells were prepared and equivalent numbers plated onto culture plastic dishes and maintained in Low-Calcium medium at 37°C during the plasma treatments. No temperature increase of the media was observed after CAP treatment. Fresh medium was added to the cells following plasma treatment. All experiments were duplicated and repeated at least twice.

Cell migration (time lapse) studies. Time-lapse studies were performed on an Olympus IX81 research microscope (Olympus America, Center Valley, PA) equipped with a Proscan motorized stage (Prior Scientific Instruments Ltd., Rockland, MA) and placed in a temperature and CO₂ controlled chamber (LiveCell Incubation System, Neue Biosciences, Camp Hill, PA). Using relief-contrast optics, images were taken every 10 minutes for 16 hours 40 minutes (100 images) for cell migration studies. Metamorph software (Molecular Devices Corporations, Chicago, IL) was used for the image analysis and the cell velocities were calculated using the cell track module in each tracked location. More detailed description can be found elsewhere¹⁶. The tracking experiment was performed immediately after treatments.

MTT assay. Cells were incubated with 1.7 µM of Thiazolyl Blue Tetrazolium Bromide (Sigma, cat#M2128) for 4 hours at 37°C. After removal of the supernatant and washing with PBS, acid isopropanol solution (isopropanol with 0.4% of 10N HCl) was added. The results were read at 570 nm on an ELISA reader.

Flow Cytometry. Flow cytometry studies were performed on a FACSCalibur DxP8 at the GWU Flow Cytometry Core Facility (manufactured by BD Biosciences and upgraded by Cytek Development). The analyzer is equipped with three lasers (providing excitation wavelengths of 488, 637 and 407 nm) and eight detectors for fluorescence.

Cell Cycle. DNA content measurement identifies G0/G1-, S- and G2/M- phases of the cell cycle, whereas EdU incorporation specifically quantifies S-phase. DNA content measurement utilized the Propidium Iodide/RNase Staining Buffer (BD Pharmingen, cat# 550825) with the addition of 0.1% Triton X-100. Cells were trypsinized with 0.25% Trypsin EDTA (Invitrogen, Gibco, cat# 25200), washed with PBS prior to fixation in 70% ethyl alcohol, stored at -20°C for 24 hours and then stained. EdU incorporation was performed with the Click-iT EdU Flow Cytometry Assay kit Alexa Fluor 647 (Invitrogen, cat# 10424) which was modified for usage with 70% ethyl alcohol fixation. Cells were incubated with 25 µM of EdU at 37°C for 1 hour prior to fixation and subsequent staining.

Drug treatment. 308 cells were incubated for ~8–9 hours at 37°C with 7 nM of Nocodazole (7 µM in DMSO stock solution, Sigma, cat# M1404), washed 2–3 times with PBS, put in fresh media, incubated for ~1–2 hours at 37°C, and then processed for further experiments.

Oxidative stress S-phase damage reporter. Phospho-Histone γH2A.X (Ser139) Rabbit Alexa Fluor 488 conjugated antibody (diluted 1:50 in 1% BSA) was used as the S-phase damage reporter (Cell Signaling Technology, cat# 9719). Rabbit (DA1E) IgG isotype control Alexa Fluor 488 conjugate (Cell Signaling Technology, cat# 2975) was used as the control antibody (also diluted 1:50 in 1% BSA).

Data analysis. The statistical analysis of data was performed by means of InStat 3 software (Graphpad Software, Inc., San Diego, CA). Data was subjected to a descriptive statistics analysis with Kolmogorov-Smirnov test for Gaussian distribution. Depending on the sample sizes, parametric or non-parametric analysis was used to determine the means and standard error of the mean (SEM), and standard deviation values. The differences between groups were determined by two tail unpaired t-tests. Data were considered significant for *p-values* < 0.05 (marked as single star), and *p-values* < 0.01 (double star) and < 0.001 (triple star) were considered as extremely significant. Flow cytometry data were analyzed with FlowJo 7.6.5 analysis software from Tree Star. Statistics from Probability Binning Comparison (Chi-Squared Test) and Kolmogorov-Smirnov Test (K-S test, $D_m - D$ maximum value and $D_{cr} - D$ critical value) indicating the confidence interval with which one can make the assertion that two flow cytometric populations are different was used for data comparison analysis²⁹. The D_{cr} -value was normalized over control populations in order to accommodate minor variations due to biological factors.

1. Lord, C. J. & Ashworth, A. The DNA damage response and cancer therapy. *Nature* **481**, 287–294 (2012).
2. Connell, P. P. & Hellman S. Advances in Radiotherapy and Implications for the Next Century: A Historical Perspective. *Cancer Res* **69**, 383–392 (2009).
3. Tsuruo, T. *et al.* Molecular targeting therapy of cancer: drug resistance, apoptosis and survival signal. *Cancer Science* **94**, 15–21 (2003).
4. Schwartz, G. K. & Shah, M. A. Targeting the Cell Cycle: A New Approach to Cancer Therapy. *J Clin Oncol* **23**, 9408–9421 (2005).



5. Keidar, M. *et al.* Cold plasma selectivity and the possibility of a paradigm shift in cancer therapy. *British Journal of Cancer* **105**, 1295–1301 (2011).
6. Vandamme, M. *et al.* ROS implication in a new antitumor strategy based on non-thermal plasma. *Int J Cancer* **130**, 2185–2194 (2012).
7. Kong, M. G. *et al.* Plasma medicine: an introductory review. *New Journal of Physics* **11**, 115012 (35pp) (2009).
8. Morfill, G. E., Shimizu, T., Steffes, B. & Schmidt, H.-U. Nosocomial infections—a new approach towards preventive medicine using plasmas. *New Journal of Physics* **11**, 115019 (2009).
9. Isbary, G. *et al.* A first prospective randomized controlled trial to decrease bacterial load using cold atmospheric argon plasma on chronic wounds in patients. *British Journal of Dermatology* **163**, 78–82 (2010).
10. Kim, K. *et al.* Atmospheric-pressure plasma-jet from micronozzle array and its biological effects on living cells for cancer therapy. *Appl Phys Lett* **98**, 073701 (2011).
11. Shashurin, A. *et al.* Influence of Cold Plasma Atmospheric Jet on Surface Integrin Expression of Living Cells. *Plasma Process. Polym.* **7**, 294–300 (2010).
12. Yan, X. *et al.* On the Mechanism of Plasma Inducing Cell Apoptosis. *IEEE Transactions on Plasma Science* **38**, 2451–2457 (2010).
13. Volotskova, O., Shashurin, A., Stepp, M. A., Pal-Ghosh, S. & Keidar, M. Plasma-controlled cell migration: localization of cold plasma-cell interaction region. *Plasma Medicine* **1**, 85–92 (2011).
14. Lippens, S., Denecker, G., Ovaere, P., Vandenabeele, P. & Declercq, W. Death penalty for keratinocytes: apoptosis versus cornification. *Cell Death and Differentiation* **12**, 1497–1508 (2005).
15. Suter, M. M. *et al.* The keratinocyte in epidermal renewal and defence. *Veterinary Dermatology* **20**, 515–532 (2009).
16. Jurjus, R. A., Liu, Y., Pal-Ghosh, S., Tadvalkar, G. & Stepp, M. A. Primary dermal fibroblasts derived from sdc-1 deficient mice migrate faster and have altered α v integrin function. *Wound Rep Reg* **16**, 649–660 (2008).
17. Hennings, H., Michael, D. & Yuspa, S. Response of carcinogen-altered mouse epidermal cells to phorbol ester tumor promoters and calcium. *J Invest Dermatol* **88**, 60–65 (1987).
18. Yuspa, S. H., Hawley-Nelson, P., Koehler, B. & Stanley, J. R. A survey of transformation markers in differentiating epidermal cell lines in culture. *Cancer Research* **40**, 4694–4703 (1980).
19. The Inverse Gaussian Distribution and Its Statistical Application—A Review, J. L. Folks and R. S. Chhikar, Page 265 of 263–289, Journal of the Royal Statistical Society. Series B (Methodological), Vol. 40, No. 3, 1978.
20. Bonner, W. M. *et al.* GammaH2AX and cancer. *Nat Rev Cancer* **8**, 957–67 (2008).
21. Marti, T. M., Hefner, E., Feeney, L., Natale, V. & Cleaver, J. E. H2AX phosphorylation within the G1 phase after UV irradiation depends on nucleotide excision repair and not DNA double-strand breaks. *PNAS* **103**, 9891–9896 (2006).
22. Zhao, H. *et al.* Induction of DNA Damage Signaling by Oxidative Stress in Relation to DNA Replication as Detected Using “Click Chemistry”. *Cytometry Part A* **79A**, 897–902 (2011).
23. Volotskova, O., Stepp, M. A. & Keidar, M. Integrin activation by a cold atmospheric plasma jet. *New Journal of Physics* **14**, 053019 (2012).
24. Haertel, B., Wende, K., von Woedtke, T., Weltmann, K.-D. & Lindequist, U. Non-thermal atmospheric-pressure plasma can influence cell adhesion molecules on HaCaT-keratinocytes. *Exp. Dermatol.* **20**, 278–96 (2011).
25. Svetlova, M. P., Solovjeva, L. V. & Tomilin, N. V. Mechanism of elimination of phosphorylated histone H2AX from chromatin after repair of DNA double-strand breaks. *Mutation Research* **685**, 54–60 (2010).
26. Ward, I. M. & Chen J. Histone H2AX Is Phosphorylated in an ATR-dependent Manner in Response to Replicative Stress. *The Journal of Biological Chemistry* **276**, 47759–47762 (2001).
27. Shashurin, A., Shneider, M. N., Dogariu, A., Miles, R. B. & Keidar, M. Temporal behavior of cold atmospheric plasma jet. *Appl Phys Lett* **94**, 231504 (1–3) (2009).
28. Shashurin, A., Shneider, M. N., Dogariu, A., Miles, R. B. & Keidar, M. Temporary-resolved measurement of electron density in small atmospheric plasmas. *Appl Phys Lett* **96**, 171502 (1–3) (2010).
29. Watson, J. Proof Without Prejudice Revisited: Immunofluorescence Histogram Analysis Using Cumulative Frequency Subtraction Plus Ratio Analysis of Means. *Cytometry* **43**, 55–68 (2001).

Acknowledgments

We'd like to thank Dr. Stuart Yuspa and his group members (National Institute of Health, NCI, Bethesda MD) for valuable discussions and help.

Author contributions

O.V. conceived and designed the experiments, performed research, analyzed the data and wrote the manuscript. T.S.H. provided assistance with designing cell cycle experiments, flow cytometry techniques and assisted in manuscript writing. M.A.S. provided assistance with designing cell migration experiments and writing the manuscript. M.K. conceived and supervised the study/project, provided assistance in manuscript writing.

Additional information

Competing financial interests: The authors declare no competing financial interests.

License: This work is licensed under a Creative Commons Attribution-NonCommercial-NoDerivative Works 3.0 Unported License. To view a copy of this license, visit <http://creativecommons.org/licenses/by-nc-nd/3.0/>

How to cite this article: Volotskova, O., Hawley, T.S., Stepp, M.A. & Keidar, M. Targeting the cancer cell cycle by cold atmospheric plasma. *Sci. Rep.* **2**, 636; DOI:10.1038/srep00636 (2012).